water

MDPI

Article

Physiological Changes and Elemental Ratio of *Scrippsiella trochoidea* and *Heterosigma akashiwo* in Different Growth Phase

Xiaofang Liu [1,†], Yang Liu [2,†], Md Abu Noman [3], Satheeswaran Thangaraj [3] and Jun Sun [3,*]

[1] Research Centre for Indian Ocean Ecosystem, Tianjin University of Science and Technology, Tianjin 300457, China; liuxiaofang@mail.tust.edu.cn
[2] Institute of Marine Science and Technology, Shandong University, Qingdao 266237, China; youngliu@mail.sdu.edu.cn
[3] College of Marine Science and Technology, China University of Geosciences, Wuhan 430074, China; abu.noman.nstu@gmail.com (M.A.N.); satheeswaran1990@gmail.com (S.T.)
* Correspondence: phytoplankton@163.com; Tel.: +86-22-6060-1116
† Xiaofang Liu and Yang Liu contributed equally to this work.

Abstract: The elemental ratios in phytoplankton are important for predicting biogeochemical cycles in the ocean. However, understanding how these elements vary among different phytoplankton taxa with physiological changes remains limited. In this paper, we determine the combined physiological–elemental ratio changes of two phytoplankton species, *Scrippsiella trochoidea* (Dinophyceae) and *Heterosigma akashiwo* (Raphidophyceae). Our results show that the cell growth period of *S. trochoidea* (26 days) was significantly shorter than that of *H. akashiwo* (32 days), with an average cell abundance of 1.21 $\times$ 10^4 cells·mL^{-1} in *S. trochoidea* and 1.53 $\times$ 10^5 cells·mL^{-1} in *H. akashiwo*. The average biovolume of *S. trochoidea* (9.71 $\times$ 10^3 μm^3) was higher than that of *H. akashiwo* (0.64 $\times$ 10^3 μm^3). The physiological states of the microalgae were assessed based on elemental ratios. The average ratios of particulate organic nitrogen (PON) to chlorophyll-a (Chl-*a*) and particulate organic carbon (POC) to Chl-*a* in *S. trochoidea* (57.32 and 168.16) were higher than those of *H. akashiwo* (9.46 and 68.86); however, the ratio of POC/PON of the two microalgae was nearly equal (6.33 and 6.17), indicating that POC/Chl-*a* may be lower when the cell is actively growing. The physiological variation, based on the POC/Chl-*a* ratio, in different phytoplankton taxa can be used to develop physiological models for phytoplankton, with implications for the marine biogeochemical cycle.

Keywords: *Scrippsiella trochoidea*; *Heterosigma akashiwo*; biovolume; chlorophyll-*a*; particulate organic nitrogen; particulate organic carbon

Citation: Liu, X.; Liu, Y.; Noman, M.A.; Thangaraj, S.; Sun, J. Physiological Changes and Elemental Ratio of *Scrippsiella trochoidea* and *Heterosigma akashiwo* in Different Growth Phase. *Water* **2021**, *13*, 132. https://doi.org/10.3390/w13020132

Received: 22 October 2020
Accepted: 3 January 2021
Published: 8 January 2021

1. Introduction

Phytoplankton is the basis of the marine food web, accounting for more than 50% of the primary production [1]. The cell size, chlorophyll-*a* (Chl-*a*) content, and elemental composition of microalgae (i.e., organic carbon and organic nitrogen) are important indicators for assessing biomass, as they have strong influences on the food web structure and the biogeochemical cycling of carbon, as well as cell growth rates [2–4]. However, these indicators vary with physical environmental parameters (i.e., irradiance and nutrient availability) and the growth phase of microalgae [5,6]. Such variations in physiological changes and elemental ratios depend on how efficiently phytoplankton biomass is remineralized by bacteria, deep ocean export flux, or utilization by consumers [7,8]. In such cases, these variations may provide a mechanistic basis for modeling phytoplankton growth, elemental ratios, and quantifying the flow energy among organisms in an ecosystem [9].

Estimation of chlorophyll is an easy technique to assess the fundamental photosynthetic performance (mainly in photosystems II) of microalgae under various environmental conditions, which reflects the photosynthetic performance of the microalgae [10]. Therefore,

it can be used as a tool to estimate phytoplankton productivity. The elemental composition of cells and the content of their constituent organic matters are two important physiological indicators for phytoplankton [11]. Particulate organic matters (POM) can influence processes such as transport, transformation, and removal of elements, which subsequently determine biological life processes and primary productivity. Thus, it is an important parameter for evaluating marine productivity [12]. Therefore, we can provide a preliminary view for evaluating the productivity of the sea based on the analysis of physiological parameters and elemental ratios.

Phytoplankton produces organic carbon by absorbing nutrients from seawater and, in turn, nutrients are returned to the seawater through remineralization. It is well-understood that studies on particulate organic carbon and nitrogen (POC/PON) have great significance for productivity modeling and the quantification of carbon in the ocean [13]. However, particulate organic nitrogen (PON) and particulate organic carbon (POC) in microalgae cells cannot be distinguished from zooplankton and non-living organic matter, so their contents are not directly available in the ocean [14,15]. Therefore, previous studies have commonly used chlorophyll content to estimate changes in intracellular carbon content, as it accurately reflects microalgae growth and photosynthetic rates [16,17]. Interestingly, the ratio between POC and Chl-*a* varies. Earlier studies have demonstrated that POC/Chl-*a* ratios are influenced by nitrogen concentrations [5]. This ratio decreases when phytoplankton are exposed to low light levels, as well as nutrient-rich zones [18,19]. Furthermore, the POC/Chl-*a* ratio has been found to be lower in an estuary, compared to the open ocean [5]. Moreover, Sathyendranath et al. studied the POC/Chl-*a* of phytoplankton using high-performance liquid chromatography (HPLC) and observed that the ratio ranged from 15 to 176 [20]. Most recent studies have examined POC/Chl-*a* and elemental content changes in phytoplankton with respect to the changes in coastal ecosystems, especially focusing on seasonal variation. However, there is scant information regarding the changes in carbon and nitrogen content during phytoplankton growth [21].

S. trochoidea (Dinophyceae) and *H. akashiwo* (Raphidophyceae) are two widely distributed harmful algal species in Chinese coastal waters. They have significant physiological differences (e.g., cell size and growth) due to variation in their taxonomic positions. Most studies have focused on growth rates and biomass under different environmental conditions, such as temperature or nutrients. For example, Qi Yu et al. studied the life history of *S.trochoidea* and found that the emergence of cysts and its reproduction rate were closely related to nitrogen concentration [22]. Furthermore, Xiao et al. pointed out a relationship between the cysts of *S. trochoidea* and vegetative cells in Daya Bay, showing that formation of cysts led to a reduction in vegetative cells [23]. Futhermore, some investigations have explained the effects of physicochemical methods for *S. trochoidea* under environmental conditions. These methods include heating, ultraviolet (UV) radiation, and others [24]. Similarly, a variation in pH also influenced the carbon assimilation and acquisition of *H. akashiwo*, along with physiological changes of growth rate [25]. Despite the fact that these studies have provided significant contributions, very few studies have examined the elemental ratios of these two important species in different stages of their growth phase [26,27].

The objective of this study was to explore the variations in POC and PON during the entire growth cycles of *S. trochoidea* and *H. akashiwo.* To accomplish this, we estimated the physiological changes (cell abundance, cell volume, Chl-*a*), element ratios (POC and PON), and inferred POC/Chl-*a* ratios from *S. trochoidea* and *H. akashiwo* during different life phases. We hope that our results provide comprehensive information on how elemental composition varies with the size difference of phytoplankton. This may be useful for marine biogeochemical modeling.

2. Material and Methods

2.1. Microalgal Species and Pre-Culture Conditions

S. trochoidea and *H. akashiwo* used in the present study were isolated, in 96-well microplates, from the coastal waters of Qinhuang Island, China. They were subsequently identified and maintained in our laboratory. Microalgal cells were cultured in f/2 medium [28] under the following culture conditions: 25 ± 1 °C; 12 h:12 h for light-dark ratio; and 200 ± 10 μmol photons m^{-2} s^{-1} for irradiance, which ensured that they were not limited by light intensity.

2.2. Determination of Microalgal Growth

Microalgae cells were collected in a sterile bench when they reached the exponential phase of growth. The collected microalgae cells were then centrifuged at 5000 rpm for 5 min and washed with sterile seawater for another 5 min for the same treatment [29]. In this way, we removed the interference of the original medium on the concentration of the new medium. The collected cells were then transferred into 2000 mL conical flasks containing 1500 mL of f/2 medium, again under the above-mentioned light conditions. The initial cell abundances of the two microalgal cell cultures were approximately 360 cells·mL^{-1} and 3000 cells·mL^{-1} at the beginning of the experiment, based on the consistent in vivo fluorescence values. Algal cells were then placed into an algal shaker with a speed of 180 rpm/min. Aliquots of approximately 100 μL of microalgae solution were transferred into a blood cell counting chamber and counted immediately using an inverted microscope (XS-213). The different growth phases of both of the considered algae were determined based on the in vivo fluorescence values and cell abundances.

2.3. Sample Analyses

Individual growth rates and doubling times of single species cultured in the laboratory were calculated based on the following equations [30]:

$$\text{Specific growth rate } (\mu, d^{-1}) = (\ln N_b - \ln N_a)/(t_b - t_a)$$

$$\text{Doubling time } (T_d, t) = \ln 2/\mu$$

where N_b and N_a denote the algal cell abundance (cells·mL^{-1}) at times t_b and t_a, respectively.

Cell volume was determined by constructing a geometric simulation graph [31]. Micrographic photos are presented in Figure 1. Chl-*a* was determined using a CE Turner Designs Fluorometer [32,33]. The PON and POC contents of the microalgae were analyzed using a Costech Elemental Analyzer (ECS4010, Milan, Italy).

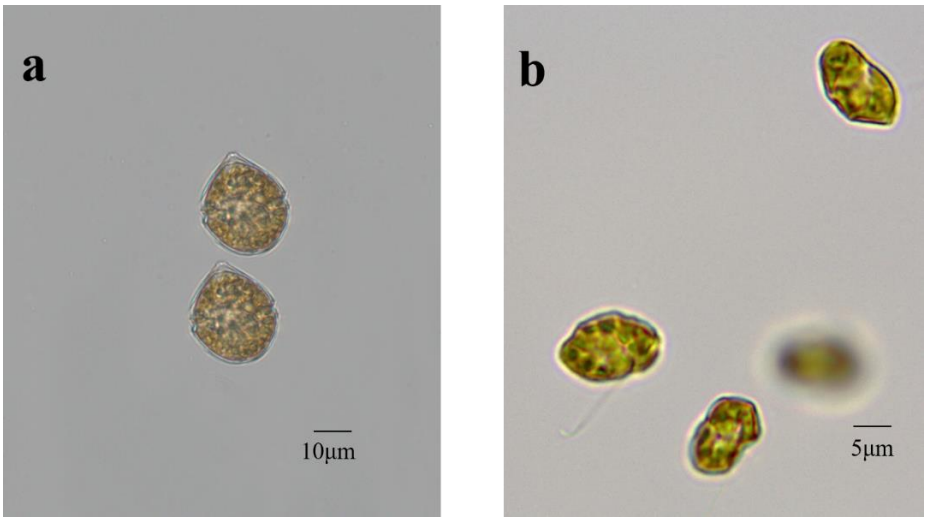

Figure 1. Light micrographic photos of two microalgae. (**a**) *S. trochoidea*; (**b**) *H. akashiwo.*

2.4. Date Analyses

All measured data are presented as mean ± standard deviation, plotted using the GraphPad Prism 8.0.2 software. Furthermore, all parameters (cell abundance, cell volume, Chl-*a*, and elements) between different species and growth phases were statistically analyzed using the SPSS software (version 21.0). Student's t-test was applied to test the differences between *S. trochoidea* and *H. akashiwo*. One-way analysis of variance (ANOVA) was used to analyze the difference of growth phases (e.g., lag, exponential, stationary, and degradation) for the two species. The levels of significance of the difference were set as $p < 0.05$ and $p < 0.01$.

3. Results

3.1. Growth Profiles of Scrippsiella trochoidea and Heterosigma akashiwo

During the experiment, the cell abundance of *S. trochoidea* significantly increased ($p < 0.01$, Figure 2a) from 360 cells·mL^{-1} to 2.60 × 10^4 cells·mL^{-1}. Similarly, the cell abundance of *H. akashiwo* also showed significant variation ($p < 0.01$, Figure 2b), from 3000 cells·mL^{-1} to 2.79 × 10^5 cells·mL^{-1}. However, the specific growth rates of *S. trochoidea* (0.86 ± 0.17 d^{-1}) and *H. akashiwo* (1.52 ± 0.38 d^{-1}) did not show any significant differences ($p > 0.05$). The doubling times of the two microalgae, *S. trochoidea* (0.80 d^{-1}) and *H. akashiwo* (0.45 d^{-1}), also had a statistically significant difference ($p < 0.05$). To simulate the growth curves of the two microalgae, the beta growth and decay model was applied in this study (Table 1). With this model, we estimated the environmental capacities of these two species as 2.19 × 10^4 cells·mL^{-1} and 2.59 × 10^5 cells·mL^{-1}, respectively (Table 1). The R^2 values of the two fitting equations were 0.87 and 0.97, respectively, illustrating good fitting results. The average cell volumes of *S. trochoidea* and *H. akashiwo* were 9.71 × 10^3 μm^3 and 0.64 × 10^3 μm^3, respectively. As shown in Figure 2c,d, a clear distinction was observed between the lag, exponential, and stationary phases ($p < 0.01$).

Table 1. The growth curve models of two microalgal species.

Species	Model	Formula	R-Squared	K (10^4·mL^{-1})	T (d)	T_m (d)
Scrippsiella trochoidea	Beta growth then decay	$Y_t = K \times (1+ (T_m - t)/(T_m - T)) \times (t/T_m)^{\wedge}(T_m/(T_m - T))$	0.872	2.185	7.21	24.09
Heterosigma akashiwo			0.970	25.88	9.55	16.60

Y_t, cell abundance during a given day; K, environmental capacity; T, time of maximum specific growth rate; T_m, time of maximum cell abundance. t, time of culture.

3.2. Chlorophyll-a Content of Two Microalgal Species

The Chl-*a* content of the two microalgae showed similar variation (Figure 2e). In both species, Chl-*a* values increased initially and then decreased. *S. trochoidea* reached a maximum of 0.43 mg·L^{-1} at day 16, whereas the higher value (1.25 mg·L^{-1}) for *H. akashiwo* was observed on day 15. Nevertheless, the Chl-*a* concentration of *H. akashiwo* was significantly higher than that of *S. trochoidea* ($p < 0.05$).

3.3. POC and PON Content in Two Microalgal Species

For *S. trochoidea* and *H. akashiwo*, the POC and PON per milliliter contents showed a similar trend, accumulating with the growth of the microalgae. The POC and PON contents of *S. trochoidea* reached their maximum range during the stationary phase, at 19.15 μg·mL^{-1} and 4.37 μg·mL^{-1} respectively. Surprisingly, a similar phenomenon occurred in *H. akashiwo*, with 85.42 μg·mL^{-1} for POC content and 10.33 μg·mL^{-1} for PON content (Figure 3a,b).

The POC content per cell of *S. trochoidea* decreased significantly during the first six days of the experiment, with a minimum value of 0.83 × 10^3 pg·cell^{-1} (exponential) and a maximum value of 3.78 × 10^3 pg·cell^{-1} (degradation) (Table 2). However, there was no significant difference between the exponential and stationary phase in terms of POC content per cell. Moreover, in terms of POC, the lag, exponential, and stationary phases were significantly lower than the degradation phase ($p < 0.05$) (Figure 3c). The lowest POC

value per cell of *H. akashiwo* was 0.12 × 10^3 pg·cell^{-1} in the stationary phase, whereas the highest value was 0.50 × 10^3 pg·cell^{-1} in the degradation of incubation (Table 2). Therefore, it is obvious that the POC value per cell of *H. akashiwo* accumulated across the degradation phase. Moreover, although the POC content per cell of *H. akashiwo* in the first three phases (lag., exp., and stat.) declined gradually, the rate of decreases was very low.

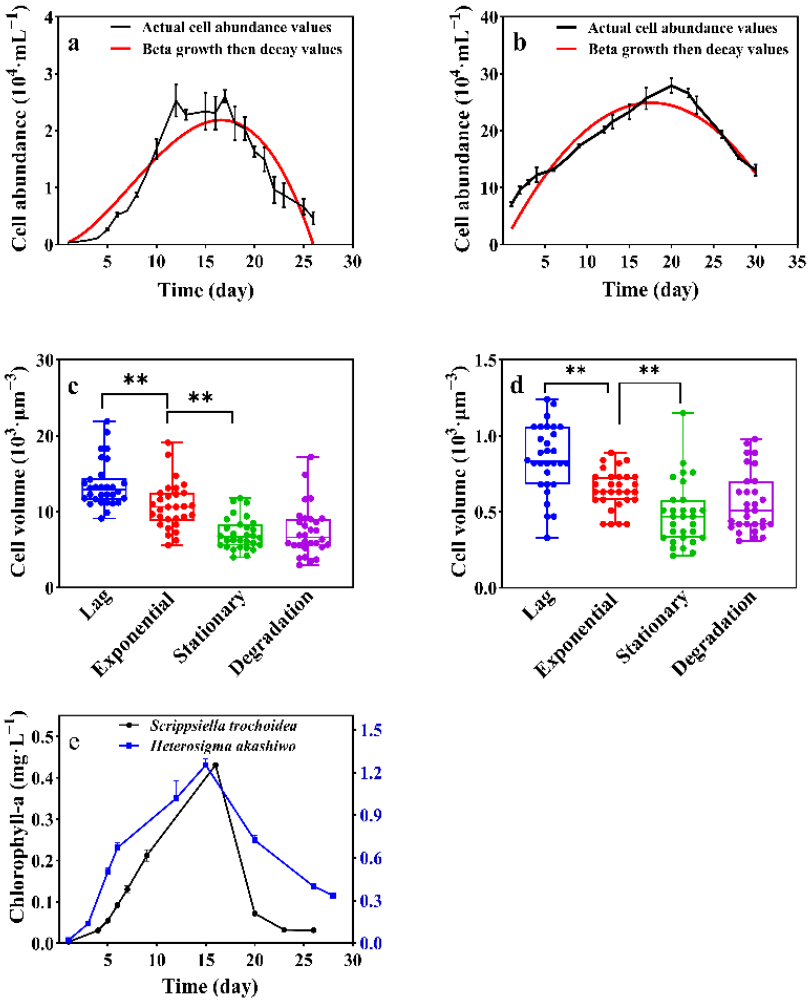

Figure 2. The growth process of *S. trochoidea* and *H. akashiwo*. (**a**) The growth curve of *S. trochoidea*; (**b**) the growth curve of *H. akashiwo*; (**c**) the cell volume of *S. trochoidea*; (**d**) the cell volume of *H. akashiwo*; (**e**) the Chl-*a* of two microalgal species; ** $p < 0.01$.

The PON content per cell of two species showed unusual differences during the experiment. The PON content per cell of *S. trochoidea* increased during the initial four days and remained relatively stable over the following 16 days, with an average value of 0.25 × 10^3 pg·cell^{-1} (Figure 3c). Similar to the POC content per cell of *H. akashiwo*, PON content accumulation occurred towards the end of the growth phase, with an average value of PON of 0.04 × 10^3 pg·cell^{-1} and a maximum of 56.66 pg·cell^{-1} (Table 2).

The PON and POC densities of the two species also showed a consistent trend. For example, the PON density in exponential and stationary phases was lower than that in the degradation phase. Interestingly, the POC density was significantly higher in the degradation phase than the other three phases ($p < 0.05$, Figure 3e,f). However, the average PON (0.03 pg·μm^{-3}) and POC (0.15 pg·μm^{-3}) density of *S. trochoidea* was lower than the PON (0.06 pg·μm^{-3}) and POC (0.40 pg·μm^{-3}) of *H. akashiwo* (Table 2).

The PON/Chl-*a* ratios of *S. trochoidea* and *H. akashiwo* had different trends throughout the growth stage, with average values of 57.32 and 9.46, respectively. The PON/Chl-*a*

ratio for *S. trochoidea* showed a maximum value on day 16, then decreased rapidly in the following days (Figure 4a). The PON/Chl-*a* ratio of *H. akashiwo* changed very little during the first 20 days and rapidly increased to 25.80 on day 26 (Figure 4b). The POC/Chl-*a* ratio of both microalgal species showed similar trends throughout the growth phases. Moreover, the POC/Chl-*a* ratio of *S. trochoidea* was significantly higher than that of *H. akashiwo*. Both *S. trochoidea* and *H. akashiwo* showed an increasing trend in POC/PON during the degradation phase, which may be due to the PON loss rate being higher than that of POC (Figure 4c).

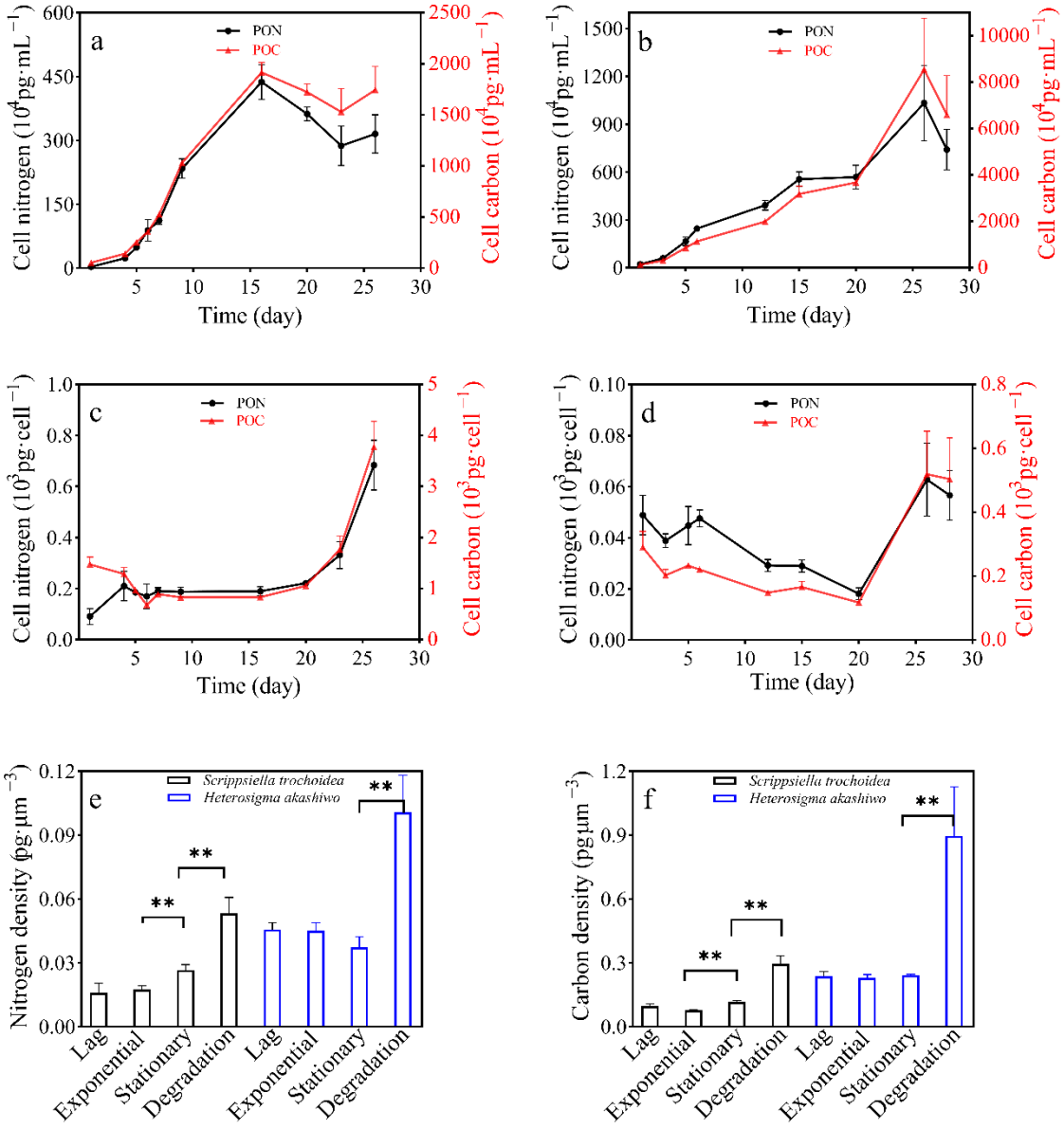

Figure 3. The organic cell composition of two species varied in different growth phases. (**a**) Cell nitrogen and carbon contents per unit milliliter of *S. trochoidea*; (**b**) cell nitrogen and carbon contents per unit milliliter of *H. akashiwo*; (**c**) nitrogen and carbon contents per unit cell of *S. trochoidea*; (**d**) nitrogen and carbon contents per unit cell of *H. akashiwo*; (**e**) cellular nitrogen density content of two species; (**f**) cellular carbon density content of two species; ** $p < 0.01$.

Table 2. Result of POC, PON quotas, and densities of two microalgal species in different growth phases.

		POC Quotas (Average ± SD) /pg·Cell^{-1}	PON Quotas (Average ± SD) /pg·Cell^{-1}	POC Densities (Average ± SD) /pg·μm^{-3}	PON Densities (Average ± SD) /pg·μm^{-3}
S. trochoidea	lag	1285.3 ± 126.55 ^{a}	210.21 ± 57.92 ^{a}	0.0947 ± 0.0093 ^{a}	0.0159 ± 0.0043 ^{a}
	exponential	825.98 ± 21.70 ^{b}	187.65 ± 18.50 ^{b}	0.0768 ± 0.0020 ^{a}	0.0175 ± 0.0017 ^{a}
	stationary	830.35 ± 41.80 ^{b}	189.60 ± 17.71 ^{b}	0.1168 ± 0.0058 ^{b}	0.0267 ± 0.0023 ^{b}
	degradation	3778.90 ± 497.56 ^{c}	683.53 ± 97.55 ^{c}	0.5101 ± 0.0671 ^{c}	0.0532 ± 0.0076 ^{c}
H. akashiwo	lag	202.18 ± 18.73 ^{a}	38.86 ± 2.73 ^{a}	0.2376 ± 0.0220 ^{a}	0.0457 ± 0.0032 ^{a}
	exponential	148.46 ± 10.00 ^{b}	29.20 ± 2.33 ^{b}	0.2298 ± 0.0155 ^{a}	0.0452 ± 0.0036 ^{a}
	stationary	116.92 ± 2.06 ^{b}	18.09 ± 2.36 ^{c}	0.2415 ± 0.0043 ^{a}	0.0374 ± 0.0049 ^{a}
	degradation	503.83 ± 129.22 ^{c}	56.66 ± 9.69 ^{a}	0.8958 ± 0.2297 ^{b}	0.1007 ± 0.0172 ^{b}

The different letter represents a significant difference in value within the same column. ($p < 0.05$).

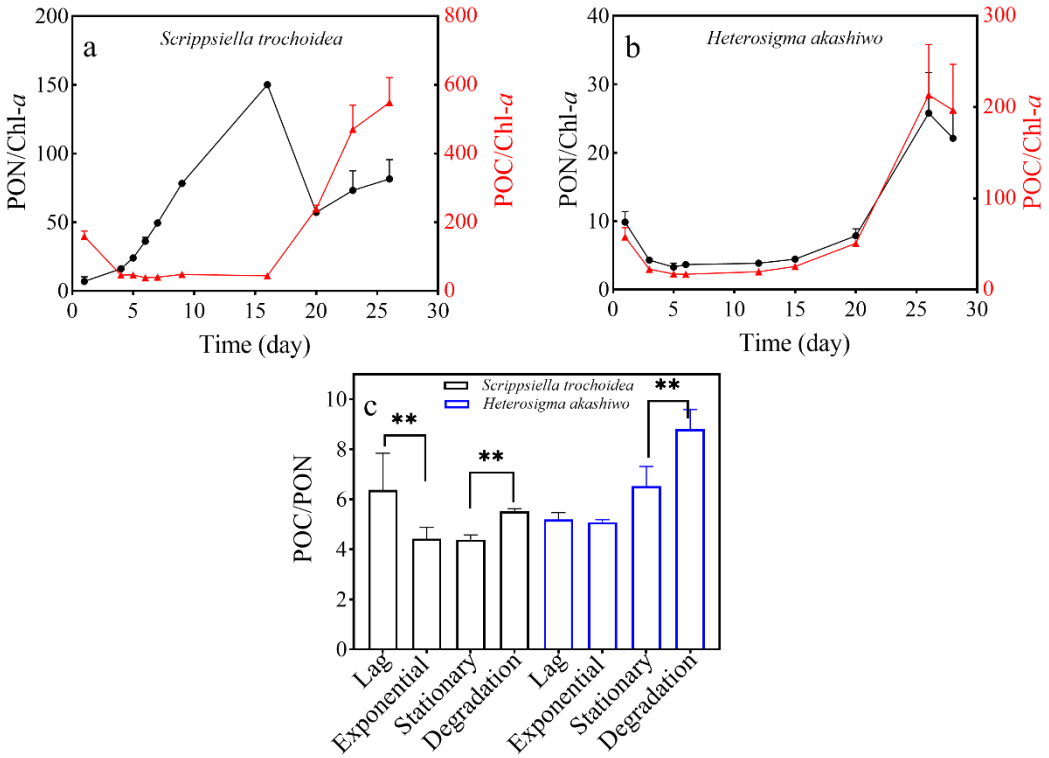

Figure 4. The change of ratios relationship for *S. trochoidea*, *H. akashiwo* in different growth phases; ** $p < 0.01$. (**a**) The ratio of PON/Chl-*a* and POC/Chl-*a* for *S. trochoidea*; (**b**) the ratio of PON/Chl-*a* and POC/Chl-*a* for *H. akashiwo*; (**c**) the ratio of POC/PON for two species.

4. Discussion

Our results showed a notable difference between the specific growth rate and cell abundance of two different phytoplankton taxa isolated from the Bohai sea. The specific growth rate results were relatively close to those of earlier reports by Xu et al. [34] and Ono et al. [35]. They noted that the maximum specific growth rate of *S. trochoidea*, under orthogonal test results, was 0.76 d^{-1} [34], while that of *H. akashiwo* did not exceed 2 d^{-1} under optimal conditions in the laboratory [35]. However, our results showed that the maximum growth rates of *S. trochoidea* and *H. akashiwo* were 0.863 d^{-1} and 1.524 d^{-1}, respectively. Interestingly, the highest abundances of *S. trochoidea* and *H. akashiwo* in this experiment were only 2.60 × 10^{4} and 2.79 × 10^{5} cells·mL^{-1}, respectively. Earlier studies have shown that, during "red tide", the cell abundances of *S. trochoidea* at Daya Bay and *H. akashiwo* at Dalian Bay reached 4.06 × 10^{4} and 72 × 10^{4} cells·mL^{-1}, respectively [23,36]. In these coastal ecosystems, the cell abundance is influenced by many environmental factors, such

as the light intensity of surface water, temperature, and nutrients. Cell abundance reaches its maximum when these environmental factors are optimal [37]. Futhermore, Daya Bay and Dalian Bay have special geographical characteristics of semi-enclosed coastal inlets, which has led to increased nutrient loading by rapidly expanding mariculture and human population growth in these regions [37,38]. However, the nutrients were depleted by microalgae during batch culture in the lab. Therefore, the cell abundances of the two microalgae species in Daya Bay and Dalian Bay were higher than those under laboratory incubation. Compared with the larger-sized *S. trochoidea* in the same culture conditions, we observed that the smaller *H. akashiwo* presented high cell abundance values. A similar phenomenon was observed, by Marañón, for the relationship between cell abundance and cell size in the surface waters of a coastal site. It has been demonstrated that cell abundance decreased with increased cell volume in different microalgae species [2]. Past studies have shown that cell size can determine the nutrient diffusion and nutrient requirements of microalgae cells. Small cells can easily maintain their growth in low-nutrient conditions [39]. Therefore, the cell abundance under large biovolume was lower than that of smaller cells in similar conditions.

Microalgae can transform inorganic matter into organic matter through photosynthesis, which plays an important role in the ocean carbon sink. In addition to Chl-*a*, intracellular carbon and nitrogen content were also used as indicators to characterize the abundances of microalgae [23]. In this experiment, the maximum Chl-*a* values of *S. trochoidea* and *H. akashiwo* were preceded by the maximum cell abundance. A similar result has been found in the varied N/P ratios of microalgae growth by past studies. The trend could be explained by good adaptation of microalgae in new experiments. This adaptation, in advance, could supply cellular substances for further proliferation [40]. Furthermore, the Chl-*a* concentration is also an important parameter for characterizing algal blooms. As the two algae in this study were isolated from Qinhuangdao Island during blooming conditions, the Chl-*a* concentration of the natural population in the coastal water likely reached a maximum before the cell abundance. Therefore, the Chl-*a* concentration exceeding a certain threshold may serve as an indicator for microalgae blooms. POC and PON content per cell of two microalgae increased in the degradation phase. As observed previously, cell division slowed down in the stationary phase, and energy began to accumulate [21,41]. For microalgae in their natural environment, the accumulated POC remains in living and non-living organisms. Eventually, it is deposited on the seafloor, thus completing the biological carbon sink [1]. In this study, the carbon content per cell of both microalgae species was reduced at the beginning of culture. Microalgae have two fundamental mechanisms of physiological characteristics in the environment, including absolute and relative adaptation [42]. Culture studies have shown that microalgae have a relative adaptation period when nutrients are not limited in a new environment, which leads to an ability to synthesize organic matter slowly for algae at the beginning of the culture [40]. Interestingly, the POC content per unit cell of *S. trochoidea* was higher than that of *H. akashiwo*, while the POC and PON density content of *S. trochoidea* were lower than those of *H. akashiwo*. We hypothesize that such variations lead to the contributions of different species to algal blooms. According to a study by Finkel et al., small cells have more elemental stoichiometry density content, which has a larger side effect than larger individuals [39]. However, Emilio et al. concluded that blooms are dominated by large, rather than small, cells [2]. Due to the large size of the cell, it has higher metabolic rates than small individuals [43]. Some observations have implied that resource acquisition and assimilation rates can be maximized by microalgae with higher biovolume. Meanwhile, they can minimize loss and material transport rates in order to survive in pelagic ecosystems [44]. Compared with large individuals, small cells have a longer growth cycle and are more easily preyed upon by consumers [45]. Based on earlier studies regarding algal bloom occurrence in the Qingdao sea, we observed that the frequency of algal blooms in this area was more severe with respect to *S. trochoidea* compared to *H. akashiwo* [46].

Therefore, compared with *H. akashiwo*, we can further extend this explanation and conclude that *S. trochoidea* may dominate the algal bloom.

The amount of carbon in phytoplankton is influenced by the cell size, as well as environmental factors [47]. However, it is difficult to directly determine the carbon biomass of phytoplankton, as zooplankton and non-living organic matter may interfere in its measurement. Therefore, it is important to estimate the biomass of phytoplankton by using the ratio of carbon to Chl-*a* content [20]. Our results suggest that the POC/Chl-*a* values of microalgae increased in the degradation phase. This is due to the depletion of nutrients while the microalgae were growing. This led to a decrease in biological activity and the accumulation of carbon content. Several studies support our findings that low values of POC/Chl-*a* exist in active microalgae cells [48]. Interestingly, we found that the POC/Chl-*a* value of *S. trochoidea* was higher than that of *H. akashiwo*. In our results, the cell biovolume tended to decrease during the growth period. In eukaryotes, renewable components, such as membranes and nucleic acids, are increased with microalgal growth. This leads to a decline in other renewable and catalytic components of the cytoplasmic proportion, such as enzyme activity and the synthesis of organic matter. Therefore, compared to larger cells, small individuals transfer nutrients to biomass at a slow rate and have low POC/Chl-*a* values [49].

The POC/PON ratio of the phytoplankton community in seawater has been found to be 106:16 [50]. However, this ratio is not consistent between lab cultures and during the process of microalgae blooming in the ocean. Although the POC/PON values for the two microalgae decreased in the exponential phase, they were close to the Redfield ratio in the degradation phase. The chemometrics of deviation states have been associated with changes in the structural elements of microalgae. Different intracellular chemometrics have different properties, which reflect differences in their ability to store intracellular nutrients during the metabolic process [51]. Mature cells can increase their allocation of nutrients in the exponential phase. Under nutrient-restricted conditions, they resynthesize substances from other parts of the cell [52]. Therefore, we observed high values during the degradation phase.

5. Conclusions

Our findings demonstrated both physiological and elemental variations in two different phytoplankton, which can serve to strengthen efforts to mechanistically quantify and assess biogeochemical processes. The similar variation of the growth curve, biomass, and elements in this study may present a useful constraint for predicting variability of phytoplankton POC, PON, POC/Chl-*a*, and PON/Chl-*a* values in cellular trait-based models. We also demonstrated taxonomic variation in POC and PON accumulation mechanisms, highlighting the impacts that biochemical traits and the biogeography of Dinophyceae and Raphidophyceae may have on ocean element patterns, which may be valuable for marine biogeochemical modeling based on Dinophyceae and Raphidophyceae.

Author Contributions: Conceptualization, J.S.; methodology, J.S.; resources, J.S.; writing—original draft preparation, X.L.; writing—review and editing, J.S., Y.L.; visualization, Y.L.; supervision, J.S.; project administration, J.S.; funding acquisition, M.A.N.; S.T. helped to modify all syntax errors of the manuscript. All authors have read and agreed to the published version of the manuscript.

Funding: This research was financially supported by the National Nature Science Foundation of China (Grant No. 41876134, 41676112 and 41276124), the Tianjin 131 Innovation Team Program (20180314), and the Changjiang Scholar Program of Chinese Ministry of Education (T2014253) to Jun Sun.

Institutional Review Board Statement: Not appicable.

Informed Consent Statement: Not appicable.

Data Availability Statement: Data is contained within the article.

Acknowledgments: This research was financially supported by the National Key Research and Development Project of China (2019YFC1407805), the National Natural Science Foundation of China (41876134, 41676112 and 41276124), the Tianjin 131 Innovation Team Program (20180314), and the Changjiang Scholar Program of Chinese Ministry of Education (T2014253) to Jun Sun.

Conflicts of Interest: The authors state that they have no conflicts of interest.

References

1. Sun, J. Marine phytoplankton and biological carbon sink. *Acta Ecol. Sin.* **2011**, *31*, 5372–5378.
2. Marañón, E. Cell size as a key determinant of phytoplankton metabolism and community structure. *Ann. Rev. Mar.* **2014**, *7*, 241–264. [CrossRef]
3. Duarte, C.M.; Conley, D.J.; Carstensen, J.; Sánchez-Camacho, M. Return to neverland: Shifting baselines affect eutrophication restoration targets. *Estuaries Coast* **2009**, *2*, 29–36. [CrossRef]
4. Longhurst, A.R.; Harrison, W.G. The biological pump: Profiles of plankton production and consumption in the upper ocean. *Prog. Oceanogr.* **1989**, *22*, 47–123. [CrossRef]
5. Jakobsen, H.H.; Markager, S. Carbon-to-chlorophyll ratio for phytoplankton in temperate coastal waters: Seasonal patterns and relationship to nutrients. *Limnol. Oceanogr.* **2016**, *61*, 1853–1868. [CrossRef]
6. Vidoudez, C.; Pohnert, G. Comparative metabolomics of the diatom *Skeletonema marinoi* in different growth phases. *Metabolomics* **2012**, *8*, 654–669. [CrossRef]
7. Laws, E.A.; Falkowski, P.G.; Smith, W.O., Jr.; Ducklow, H.; McCarthy, J.J. Temperature effects on export production in the open ocean. *Glob. Biogeochem. Cycles* **2000**, *14*, 1231–1246. [CrossRef]
8. Armstrong, R.A.; Lee, C.; Hedges, J.I.; Honjo, S.; Wakeham, S.G. A new, mechanistic model for organic carbon fluxes in the ocean based on the quantitative association of POC with ballast minerals. *Deep Sea Res. Part II* **2001**, *49*, 219–236. [CrossRef]
9. Vrede, K.; Heldal, M.; Norland, S.; Bratbak, G. Elemental composition (C, N, P) and cell volume of exponentially growing and nutrient-limited bacterioplankton. *Appl. Environ. Microbiol.* **2002**, *68*, 2965–2971. [CrossRef]
10. Markou, G.; Depraetere, O.; Muylaert, K. Effect of ammonia on the photosynthetic activity of Arthrospira and Chlorella: A study on chlorophyll fluorescence and electron transport. *Algal Res.* **2016**, *16*, 449–457. [CrossRef]
11. Bopaiah, B.; Benner, R. Carbon, nitrogen, and carbohydrate fluxes during the production of particulate and dissolved organic matter by marine phytoplankton. *Limnol. Oceanogr.* **1997**, *42*, 506–518. [CrossRef]
12. Liang, C.J.; Wang, J.T.; Tan, L.J. Distribution of particulate organic carbon in Qingdao coastal waters in summer and winter. *Mar. Environ. Sci.* **2010**, *29*, 12–16. [CrossRef]
13. Mongin, M.; Nelson, D.M.; Pondaven, P.; Tréguer, P. Simulation of upper-ocean biogeochemistry with a flexible-composition phytoplankton model: C, N and Si cycling and Fe limitation in the Southern Ocean. *Deep Sea Res. Part II* **2006**, *53*, 601–619. [CrossRef]
14. Eppley, R.W.; Chavez, F.P.; Barber, R.T. Standing stocks of particulate carbon and nitrogen in the equatorial Pacific at 150 W. *J. Geophys. Res. C: Ocean.* **1992**, *97*, 655–661. [CrossRef]
15. Oubelkheir, K.; Claustre, H.; Sciandra, A.; Babin, M. Bio-optical and biogeochemical properties of different trophic regimes in oceanic waters. *Limnol. Oceanogr.* **2005**, *50*, 1795–1809. [CrossRef]
16. Behrenfeld, M.J.; Boss, E.; Siegel, D.A.; Shea, D.M. Carbon-based ocean productivity and phytoplankton physiology from space. *Glob. Biogeochem.* **2005**, *19*, GB1006. [CrossRef]
17. Platt, T.; Sathyendranath, S.; Forget, M.H.; White, G.N., III; Caverhill, C.; Bouman, H. Operational estimation of primary production at large geographical scales. *Remote Sens. Environ.* **2008**, *112*, 3437–3448. [CrossRef]
18. Terry, K.L.; Hirata, J.; Laws, E.A. Light-limited growth of two strains of the marine diatom *Phaeodactylum tricornutum* Bohlin-Chemical composition, carbon partitioning and the diel periodicity of physiological processes. *J. Exp. Mar. Biol. Ecol.* **1983**, *68*, 209–227. [CrossRef]
19. Markager, S.; Sand-Jensen, K. Implications of thallus thickness for growth-irradiance relationships of marine macroalgae. *Eur. J. Phycol.* **1996**, *31*, 79–87. [CrossRef]
20. Sathyendranath, S.; Stuart, V.; Nair, A.; Oka, K.; Nakane, T.; Bouman, H.; Platt, T. Carbon-to chlorophyll ratio and growth rate of phytoplankton in the sea. *Mar. Ecol. Prog. Ser.* **2009**, *383*, 73–84. [CrossRef]
21. Massie, T.M.; Blasius, B.; Weithoff, G.; Gaedke, U.; Fussmann, G.F. Cycles, phase synchronization, and entrainment in single-species phytoplankton populations. *Proc. Natl. Acad. Sci. USA* **2010**, *107*, 4236–4241. [CrossRef]
22. Qi, Y.Z.; Zheng, L.; Wang, R. The life cycle of *Scrippsiella trochoidea* and its physiol-ecological control. *Chin. J. Oceanol. Limnol* **1997**, *28*, 588–593.
23. Xiao, Y.Z. The relationship between *Scrippsiella trochoidea* red tide and cysts in the Daya Bay. *Mar. Sci.* **2001**, *25*, 50–54.
24. Wang, Z.H.; Liang, W.B.; Guo, X.; Liu, L. Inactivation of *Scrippsiella trochoidea* cysts by different physical and chemical methods: Application to the treatment of ballast water. *Mar. Pollut. Bull.* **2018**, *126*, 150–158. [CrossRef] [PubMed]
25. Liu, Y.; Lou, Y.D.; Wang, H.X.; Liu, Q. Effects of carbon source restricted on pH chang during growth of red tides algae. *Mar. Environ. Sci.* **2019**, *38*, 286–293.
26. Zhou, C.X.; Wang, F.X.; Yan, X.J. Effects of temperature, salinity and irradiance on the cell stability of *Heterosigma akashiwo* Hada. *Mar. Environ. Sci.* **2008**, *27*, 17–20. [CrossRef]

27. Qin, X.M.; Qin, P.Y.; Zou, J.Z. Effects of nitrogen and phosphorus on the growth of a red tide dinoflagellate *Scrippsiella trochoidea* (stein) loeblch III. *Chin. J. Oceanol. Limnol.* **1999**, *17*, 212–218. [CrossRef]
28. Guillard, R.R.L.; Hargraves, P.E. Stichochrysis immobilis is a diatom, not a chrysophyte. *Phycologia* **1993**, *32*, 234–236. [CrossRef]
29. Liu, Y.; Lv, J.P.; Feng, J.; Liu, Q.; Nan, F.R.; Xie, S.L. Treatment of real aquaculture wastewater from a fishery utilizing phytoremediation with microalgae. *J. Chem. Technol. Biotechnol.* **2019**, *94*, 900–901. [CrossRef]
30. Sun, J.; Ning, X.R. Marine phytoplankton specific growth rate. *Adv. Earth Sci.* **2005**, *20*, 939–945. [CrossRef]
31. Sun, J.; Liu, D.Y. Geometric models for calculating cell biovolume and surface area for phytoplankton. *J. Plankton Res.* **2003**, *25*, 1331–1346. [CrossRef]
32. Welschmeyer, N.A. Fluorometric analysis of chlorophyll *a* in the presence of chlorophyll *b* and pheopigments. *Limnol. Oceanogr.* **1994**, *39*, 1985–1992. [CrossRef]
33. Liu, H.J.; Xue, B.; Feng, Y.; Zhang, R.; Chen, M.; Sun, J. Size-fractionated Chlorophyll a biomass in the northern South China Sea in summer 2014. *Chin. J. Oceanol. Limnol.* **2016**, *34*, 672–682. [CrossRef]
34. Xu, N.; Lv, S.H.; Chen, J.F.; He, L.S.; Xie, L.C.; Qi, Y.Z. The influence of water temperature and salinity on the growth of *Scrippsiella trochoidea*. *Mar. Environ. Sci.* **2004**, *23*, 36–38. [CrossRef]
35. Ono, K.; Khan, S.; Onoue, Y. Effects of temperature and light intensity on the growth and toxicity of *Heterosigma akashiwo* (Raphidophyceae). *Aquacult. Res.* **2000**, *31*, 427–433. [CrossRef]
36. Guo, Y.J. Studies on *heterosigma akashiwo* (HADA) in the Dalian bight, Liaoning, China. *Oceanol. Limnol. Sin.* **1994**, *25*, 211–215.
37. Wang, Z.H.; Qi, Y.Z.; Chen, J.F.; Xu, N.; Yang, Y.F. Phytoplankton abundance, community structure and nutrients in cultural areas of Daya Bay, South China Sea. *J. Mar. Syst.* **2006**, *62*, 85–94. [CrossRef]
38. Wang, H.Q. The *Heterosigma Akashiwo* red tide and ecological characteristics in Dalian Bight. *Res. Environ. Sci.* **1991**, *4*, 53–59.
39. Finkel, Z.V.; Beardall, J.; Flynn, K.J.; Quigg, A.; Rees, T.A.V.; Raven, J.A. Phytoplankton in a changing world: Cell size and elemental stoichiometry. *J. Plankton Res.* **2009**, *1*, 119–137. [CrossRef]
40. Sun, J.; Liu, D.Y.; Chen, Z.T.; Wei, T.D. Growth of *Platymonas helgolandica var. tsingtaoensis*, *Cylindrotheca closterium* and *Karenia mikimotoi* and their survival strategies under different N/P ratios. *J. Appl. Ecol.* **2004**, *15*, 2122–2126. [CrossRef]
41. Goldman, J.C.; Hansell, D.A.; Dennett, M.R. Chemical characterization of three large oceanic diatoms: Potential impact on water column chemistry. *Mar. Ecol. Prog. Ser.* **1992**, *88*, 257–270. [CrossRef]
42. Beardall, J.; Allen, D.; Bragg, J.; Finkel, Z.V.; Flynn, K.J.; Quigg, A.; Raven, J.A. Allometry and stoichiometry of unicellular, colonial and multicellular phytoplankton. *New Phytol.* **2009**, *181*, 295–309. [CrossRef]
43. Riegman, R.; Mur, L.R. Theoretical considerations on growth kinetics and physiological adaptation of nutrient-limited phytoplankton. *Arch. Microbiol.* **1984**, *140*, 96–100. [CrossRef]
44. Huete-Ortega, M.; Cermeno, P.; Calvo-Díaz, A.; Marañón, E. Isometric size-scaling of metabolic rate and the size abundance distribution of phytoplankton. *Proc. R. Soc. Lond. Ser. B* **2012**, *279*, 1815–1823. [CrossRef]
45. Sunda, W.G.; Hardison, D.R. Evolutionary tradeoffs among nutrient acquisition, cell size, and grazing defense in marine phytoplankton promote ecosystem stability. *Mar. Ecol. Prog. Ser.* **2010**, *401*, 63–76. [CrossRef]
46. Bian, M.M.; Song, J.L.; Feng, J.Y.; Liu, Z.L. Occurrence and ananlysis of red tides in Qinhuangdao sea area. *Heibei Fish.* **2019**, *8*, 26–28.
47. Viličić, D. An examination of cell volume in dominant phytoplankton species of the central and southern Adriatic Sea. *Int. Rev. Gesamten Hydrobiol.* **1985**, *70*, 829–843. [CrossRef]
48. Parsons, T.R.; Stephens, K.; Strickland, J.D.H. On the chemical composition of eleven species of marine phytoplankters. *J. Fish. Res. Board Can.* **1961**, *18*, 1001–1016. [CrossRef]
49. Marañón, E.; Cermeño, P.; López-Sandoval, D.C.; Rodríguez-Ramos, T.; Sobrino, C.; Huete-Ortega, M.; Maria Blanco, J.; Rodríguez, J. Unimodal size scaling of phytoplankton growth and the size dependence of nutrient uptake and use. *Ecol. Lett.* **2013**, *16*, 371–379. [CrossRef]
50. Geider, R.; La Roche, J. Redfield revisited: Variability of C: N: P in marine microalgae and its biochemical basis. *Eur. J. Phycol.* **2002**, *37*, 1–17. [CrossRef]
51. Klausmeier, C.A.; Litchman, E.; Levin, S.A. Phytoplankton growth and stoichiometry under multiple nutrient limitation. *Limnol. Oceanogr.* **2004**, *49*, 1463–1470. [CrossRef]
52. Arrigo, K.R. Marine microorganisms and global nutrient cycles. *Nature* **2005**, *437*, 349–355. [CrossRef] [PubMed]